EIGHTH EUROPEAN ROTORCRAFT FORUM

Paper No. 12.3

IMPORTANCE OF HELICOPTER PERFORMANCE TO AIR-TO-AIR COMBAT

Michael Falco
Grumman Aerospace Corporation
Bethpage, New York, USA

and

Dr. Roger Smith
U.S. Army Aviation Research and Development Command
St. Louis, Missouri, USA

August 31 through September 3, 1982

AIX-EN-PROVENCE, FRANCE

ASSOCIATION AERONATIQUE ET ASTRONAUTIQUE DE FRANCE

ABSTRACT

A computational investigation was conducted to quantify the impact of maneuver and maximum speed performance on the combat effectiveness of current and advanced design helicopters in one-on-one engagements against specific threats. A newly developed procedure employing a stochastic learning method in conjunction with dynamic simulation of helicopter flight and weapon system operation was used to derive helicopter maneuvering strategies. The derived strategies maximize either survival or kill probability and are in the form of a feedback control based upon threat visual or warning system cues. Maneuverability parameters implicit in the strategy development included maximum longitudinal acceleration and deceleration, maximum sustained and transient load factor turn rate at forward speed, and maximum pedal turn rate and lateral acceleration at hover. Results are presented in terms of probability of kill for all combat initial conditions for two air-to-air threat categories. In the first category the use of maneuverability is examined in a defensive role against an anti-tank guided missile (ATGM) launched by a threat helicopter. The second is concerned with the impact of maneuverability in both defensive and offensive roles against a gun armed helicopter threat.

1. INTRODUCTION

In the early stages of military helicopter conceptual design, there is a need for methodology to better quantify combat effectiveness in terms of the major aircraft/weapon system attributes such as design maneuver capability and maximum speed, weapon capability, passive/active survivability equipment performance, detectability, and threat warning. To analyze the maneuver capability contribution to combat effectiveness against various threats, the associated models are required to be of high fidelity in terms of the dynamical simulation of helicopter flight and yet permit the maneuver contribution to be assessed either singly or in concert with the other system attributes in an equally detailed way. It is necessary for the methodology to develop an optimal probability of kill or survival solution for all relative geometries for which combat can be initiated. Solution optimality is important for consistent effectiveness comparisons between aircraft/weapon concepts and serves to minimize the effect of maneuver strategy prejudgments and other preliminary bias factors introduced by the analyst.

Application of modern optimal control and differential game theory methods seems well suited to these problems at first sight. However, the pioneering effort of Isaacs (Ref. 1), followed by those of Breakwell and Merz (Ref. 2), indicate that there does not appear to be a general systematic method for solution of even some simply structured pursuit-evasion games. This difficulty has led applications oriented investigators (Ref. 3, 4, 5) toward consideration of discrete game approximations which circumvent the analytical problems of the continuous theory, and still offer some form of suboptimal solution in more realistic combat models.

This paper presents a partial summary of recent computational experience gained in military helicopter design applications using variations of a stochastic learning method first reported in Ref. 4. Representative computational results are presented for two important categories of one-on-one helicopter air combat: the first, a study of maneuver capability in defending against an anti-tank guided missile (ATGM) launched by a threat helicopter; the second, maneuverability employed defensively and offensively against a gun-armed threat helicopter. An explanation of the maneuver strategy development and effectiveness assessment methodology is given in both case studies. The representative results reported here limit helicopter maneuvering to constant altitude flight paths; solutions using variable altitude maneuvering with terrain constraints in the air-to-air gun study were not available in time for inclusion in this publication. Geographical terrain features have not been considered in these studies; the ground is modeled as a plane.

The same approach has been extended to problems of land warfare, particularly armored vehicle maneuver effectiveness and survivability against anti-tank missile threats. Corroboration of the computer derived solutions for specific threat cases has been obtained in inde pendent field trials with the actual systems. Additional effort must be dedicated to flight trial verification of the model approximations and computed solutions. Continued research is warranted in the application of optimal control, differential game, and the stochastic processes branches of applied mathematics to provide effective numerical procedures for helicopter combat analyses.

2. PERFORMANCE IN AIR-TO-AIR MISSILE AVOIDANCE

2.1 MISSILE THREAT

The threat is an optically tracked, wire guided missile employing a semi-automatic command to line of sight guidance system. This threat was primarily designed as an anti-tank guided missile (ATGM), but has air-to-air application as well. It is assumed to have a 245 m/s sustainer velocity, maximum range of 4 km, and maximum flight time of 16.3 s. In addition, it is assumed to have a 4 g maximum lateral maneuver capability, and that the launch aircraft is at co-altitude with the target. The low combat flight altitude of the target (dictated by detection and masking considerations) allows the survivability results to be safely extrapolated to ground launched cases as well. This threat is normally equipped with a shaped-charge contact fuze warhead for armor penetration. However, proximity fuze warheads employing expanding rod or fragment kill mechanisms are also indicated to be adaptable to this missile airframe, and two of these types were considered in this investigation. The contact fuze warhead lethality model utilizes a probability of kill, $P_K = 1.0$ for missile contact anywhere on the helicopter fuselage envelope. Two proximity fuze warhead models are described in Fig. 1. Warhead A denotes an expanding rod warhead as used in short range air-to-air missiles. Warhead B is the

largest blast/fragment warhead that can be accommodated by the missile airframe and propulsion configuration. The kill effectiveness, P_K, of these two warheads is given as a function of detonation distance R_{DET} (from the target cg). The data shown represent an average of all warhead/target detonation aspects; however, functional dependence upon aspect is considered in the studies.

2.2 THREAT WARNING AND MANEUVER STRATEGY

Earlier investigations have postulated the need for evading aircraft to be equipped with a threat warning system in order to achieve a reasonable measure of survivability against missile threats. The aircraft in this investigation is assumed to employ an active radar warning system supplying relative range and azimuth information regarding the incoming threat. The baseline configuration for this warning receiver model employs 12 azimuth gates and 7 range gates from 0.25 km out to a maximum detection range of 5 km, as shown in Fig. 2. This configuration is indicative of the warning receiver performance levels that are projected for operational systems in the near future.

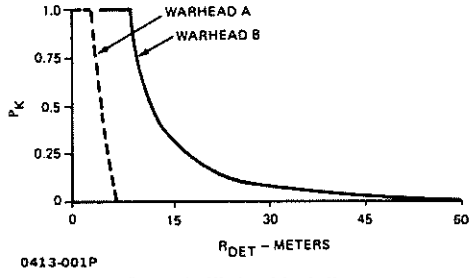

Figure 1. Warhead Lethality

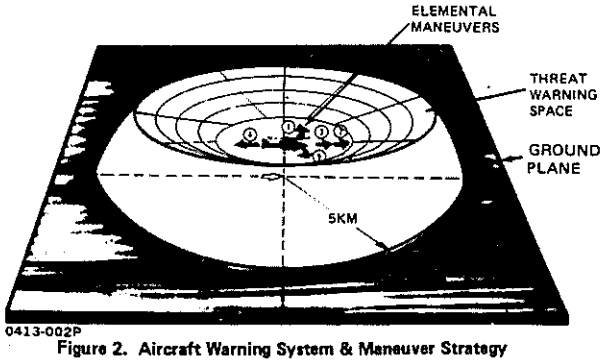

Figure 2. Aircraft Warning System & Maneuver Strategy

At each threat warning contingency (represented by one of the 7 x 12 = 84 range/azimuth cells), the aircraft is allowed a choice from a finite number of elemental maneuvers. Five elemental maneuver choices are shown in Fig. 2. The choices may be comprised of maximum performance turns, longitudinal acceleration, deceleration, and a straight ahead constant speed policy. In vertical plane maneuvering studies climb and pushover maneuver choices would be added. An aircraft evasive maneuvering strategy is the selection of an elemental maneuver for each threat warning cell. An optimal strategy is a strategy which maximizes aircraft survivability for all launch initial conditions.

2.3 STOCHASTIC LEARNING METHOD

The stochastic learning method is comprised of two phases: a reinforcement learning phase, in which the optimized evasive strategy is ultimately derived, and a statistics phase. The learning phase involves the development of a decision table that consists of a probability distribution used in the selection of an elemental maneuver for each warning contingency. That table is shown in its initial form at the upper right of Fig. 3. The column indices 1, ..., 5 under the control caption are the five elemental maneuver choices. The row indices, labled R, ranging from 1, ..., 84 represent the threat warning contingencies. Initially, the choice of maneuver for each contingency is governed by sampling from the equally likely discrete distribution, as shown.

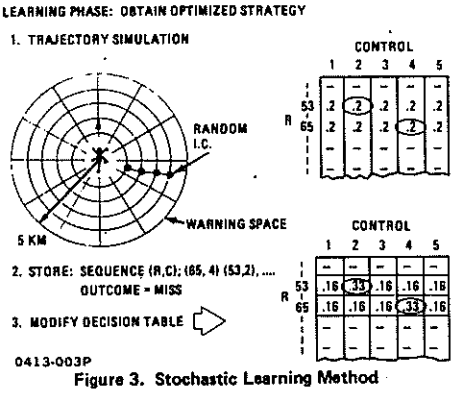

Figure 3. Stochastic Learning Method

A random initial condition for the combat is selected and both aircraft and threat trajectories dynamically simulated. The aircraft employs a selected maneuver within the initial contingency cell until a second cell is entered and another maneuver choice is made. Threats may be launched outside the range of the warning space. In this case, the aircraft maintains its current speed and heading until the threat first enters the warning space at which time the control selection process begins. This simulation process is continued until warhead detonation or flyby, and a kill or survival event is calculated using the probability of kill distribution derived from the warhead lethality function. In the process of simulating the trajectories, the sequential contingency/control pairs employed by the aircraft are temporarily stored. Based upon the kill/survival event, the probability associated with those control choices made for each contingency are modified by a reinforcement rule. For the survival event, the probability of employing the same elemental maneuver for each stored contingency is increased, and is decreased for the kill event. The trajectory simulation and table modification process is repeated over all possible threat launch range and azimuth initial conditions using a random selection method. Approximately 100 launches per warning cell or 8400 total trajectories are numerically simulated to produce a converged decision table. The 8400 trajectories require approximately 20 minutes CPU time on IBM 370/168 systems.

In the statistics phase the converged decision table is fixed. Random starting conditions are then selected and trajectories dynamically simulated. In a manner typical of Monte Carlo approaches, the averaged probability of kill and missile warhead detonation distance statistics are computed for each warning (or launch) cell.

2.4 ELEMENTAL MANEUVERS

In this paper, the helicopter maneuver choices are restricted to those which maintain a low constant altitude. The maneuver vectorgram, labeled control set I in Fig. 4, is aimed at quantifying the impact of longitudinal and turn maneuver capability in constructing an effective evasive maneuvering strategy throughout the whole speed range from hover to maximum level flight speed. At forward speed, the helicopter can command maximum transient (or sustained) load factor turns, labeled (1) and (5); maximum longitudinal acceleration, (2); or maximum longitudinal deceleration, (4); as well as maintaining the current speed and heading, (3). At very low forward speeds including hover, the load factor turns are replaced with maximum rate pedal turns. The maneuver vectorgram at the right in Fig. 4, captioned control set II, is aimed at quantifying the impact of lateral acceleration (sideward flight) and pedal turn capability in constructing a maneuver strategy at or near hover speeds only. Choices (1) and (5) represent maximum performance pedal turns; choices (2) and (4), maximum performance lateral accelerations; and choice (3) maintains current lateral speed at the current aircraft heading. Similarly, vertical or composite vertical/horizontal maneuver models can be constructed and investigated without change in the basic methodology.

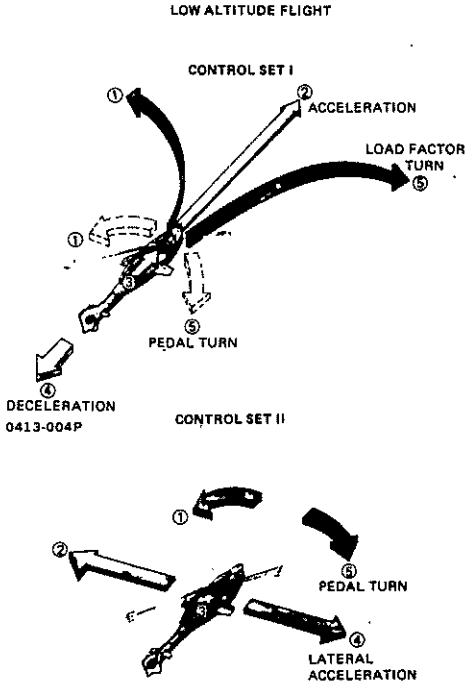

Figure 4. Elemental Maneuvers

2.5 HELICOPTER MAXIMUM MANEUVER CAPABILITY

Figure 5 graphically summarizes the sea level maximum maneuver capability data associated with the elemental maneuver models of Fig. 4, for a conceptual enhanced performance version of a current helicopter design. The maximum commanded turn capabilities shown at upper left are employed for choices (1) and (5) in control sets I and II. For the case of maximum transient turn, the associated longitudinal transient deceleration is shown at the upper right. The maximum longitudinal acceleration and deceleration capabilities utilized for choices (2) and (4) in control set I, are given in the two lower diagrams. The lateral acceleration required for choices (2) and (4) of control set II is given in the diagram at lower left. These studies employ first order models for the aircraft transient response to the maximum acceleration and rate commands.

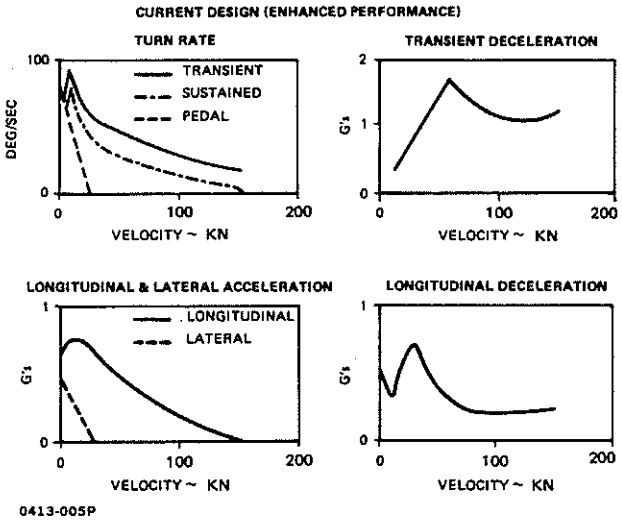

Figure 5. Maximum Maneuver Capability

2.6 EFFECTIVENESS OF MANEUVER PERFORMANCE

The aircraft survivability or equivalently the missile kill effectiveness results (P_K) for the ATGM threat for all launch conditions are calculated and presented in the helicopter warning space coordinate system for convenience. In this case the maximum effective launch range of the threat (4 km) was less than the maximum detectable range of the warning system (5 km). (The results could also be presented in a space relative to the launch aircraft and would represent the effective launch envelope for that missile against an optimally maneuvered evader.) Threat launches were initiated from 72 of the 84 range/azimuth cells within the 5 km maximum range in both learning and statistics phases. No launches were simulated from the 12 cells making up the inner range ring (range less than 0.25 km) due to severe missile guidance transients at very short target ranges. It should be noted that in all results presented, the attacking aircraft is assumed to maintain a speed equal to the initial speed of the target, and fly a pure pursuit navigation course toward the target during missile flyout.

Figure 6 shows the kill effectiveness of the ATGM equipped with the expanding rod type war head. Because of left-right symmetry considerations, only half of the warning space need be shown. Four levels of kill effectiveness (P_K) are given to simplify the presentation. The legend at lower center is employed throughout this section. The origin of each semicircular plot corresponds to the helicopter position at missile launch, and the aircraft initial heading (0°) is shown by the helicopter symbol. Head on launches correspond to 0° to 30° azimuth sectors, and tail aspects launches 150° to 180°, respectively. The kill results are presented for four helicopter initial speed condition groups, beginning with hover at upper left, and progressing clockwise to maximum speed at the lower left. Within each of the four speed groups, the left semicircle, labeled nonmaneuver, represents missile kill effectiveness when the aircraft maintains its current speed and heading. This case is important for quantifying target speed effects without maneuver, and is useful for establishing baseline survivability measures without use of threat warning and optimal maneuver. Clearly, a scan of the nonmaneuver cases for the four initial speeds indicates improving survivability in longer range rear aspect launches with increasing speed, but at the expense of reduced survivability in the corresponding forward launch cases. In addition, a small window of improving survivability for short range beam launch cases can be seen developing with increased speed; this is due to guidance transients associated with high line of sight rate targets. The nonmaneuver cases show that speed alone (equivalent to no threat warning) does not provide sufficient survivability against the ATGM with Warhead A. The semicircles labeled

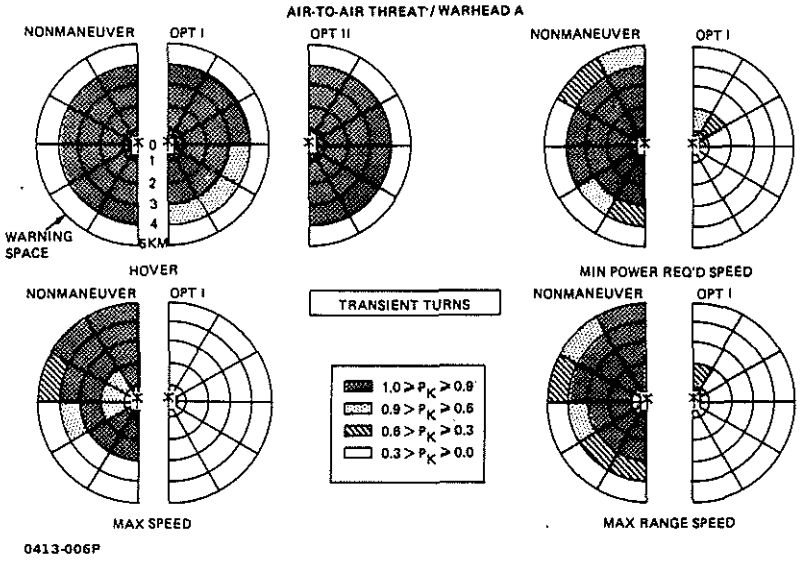

Figure 6. Helicopter Survivability

OPT I in each of the four speed groups quantifies the survivability improvements that can be achieved with the 84 cell warning system, together with an optimal maneuvering strategy derived from control set I. In the four results labeled OPT I, the helicopter employed its maximum transient load factor turn performance for choices (1) and (5). One can see that survivability is still poor with combat initiated at hover, although small improvements exist for tail launches at the 4 km range. This is due to helicopter acceleration away from the oncoming missile and the missile maximum range limitation. However, at higher initial speeds, optimal maneuvering, employing transient load factor performance can provide high survivability. The lack of effectiveness of control set II (lateral acceleration and pedal turns) in constructing an optimal maneuver strategy from hover is shown by the shaded semi-circle labeled OPT II. This result, together with that for OPT I to the immediate left, indicate the low survivability afforded by maneuver against the ATGM with Warhead A at hover flight speeds.

The sensitivity of survivability of the enhanced performance helicopter to variations in ATGM warhead type and lethality is shown in Fig. 7. The three warhead types: contact, proximity Warhead A, and proximity Warhead B, have been examined at the helicopter minimum power required initial speed. The helicopter employs control set I with maximum transient turns for elemental maneuvers (1) and (5) in the optimal strategy development. The nonmaneuver and optimal survivability results for Warhead A are repeated at lower left.

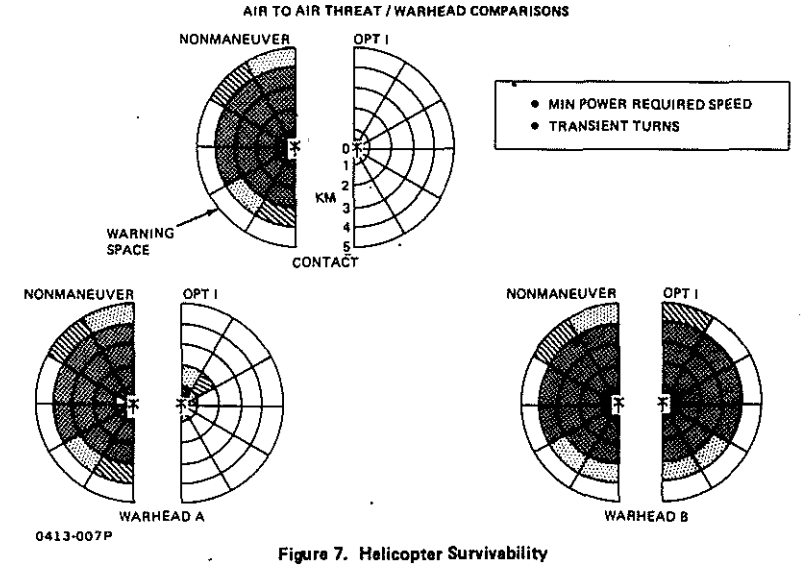

Figure 7. Helicopter Survivability

Corresponding survivability results for the contact fuzed warhead are shown upper center; those for Warhead B are shown at the lower right. The nonmaneuver results are statistically equivalent in all cases and typify the small miss distances achievable by the missile guidance system against constant velocity targets. The helicopter can be made completely survivable against the contact fuzed ATGM using optimal maneuvering at this initial aircraft speed. However, the corresponding result for Warhead B indicates that optimal maneuver would be completely ineffective. These results indicate the strong interplay between missile warhead lethality and guidance, and the need for carefully timed deployment of the aircraft's maximum maneuver capability to generate adequate miss distances against this threat.

Three optimal evasive trajectories from hover using maneuver set I against the contact fuzed warhead are shown in Fig. 8. The survivability results for nonmaneuver and optimal maneuver are presented at the upper left of the figure. For each case illustrated, only the terminal portion of the missile path and the entire helicopter path are shown because of scale effects. The head on case at upper right and beam aspect case at lower right illustrate pedal turns immediately following launch, followed by straight accelerated flight and finally, a maximum performance load factor turn near termination. The tail aspect launch at lower left employs only the acceleration segment followed by the load factor turn at termination. In all cases shown, the aircraft maneuvers to achieve a tail aspect to present its minimal fuselage envelope dimension at missile flyby. Launches within 2 km cannot be made highly survivable because the missile flight time is too short to permit adequate forward acceleration and load factor turn maneuvers to avoid fuselage hits.

3. PERFORMANCE IN AIR-TO-AIR GUN COMBAT

This section concerns quantifying the impact of aircraft maneuverability, gun capability and ballistic hardening in air-to-air visual range gun combat. Three blue (friendly) helicopter design concepts are separately evaluated against the same red (threat) helicopter. The first blue aircraft, called the baseline, is representative of a current operational attack helicopter design, and the second, an advanced light helicopter concept (LHX) having greater maximum maneuver capability and level flight speed. The third concept aircraft is a variant of the second; employing equivalent maneuverability but with improved ballistic hardening.

3.1 VISUAL MODEL

The visual model employed in the gun combat studies is displayed in Fig. 9. Each combatant is assumed to have a visual contact volume extending to a maximum range of visual detectability. Within this volume each combatant is permitted to select a maximum performance tactical maneuvering strategy for flight path control of the aircraft. For these studies the maximum range has been arbitrarily set at 3 km for both combatants. This is consistent with line of sight visual capabilities at low altitudes in typical rolling terrains. Aircraft size, paint/camouflage, and background contrast factors have been neglected. A helmet mounted sight operational tracking volume associated with a turreted gun fire control system is also considered as illustrated. Gun firing opportunities exist only when the target is within the tracking volume limits.

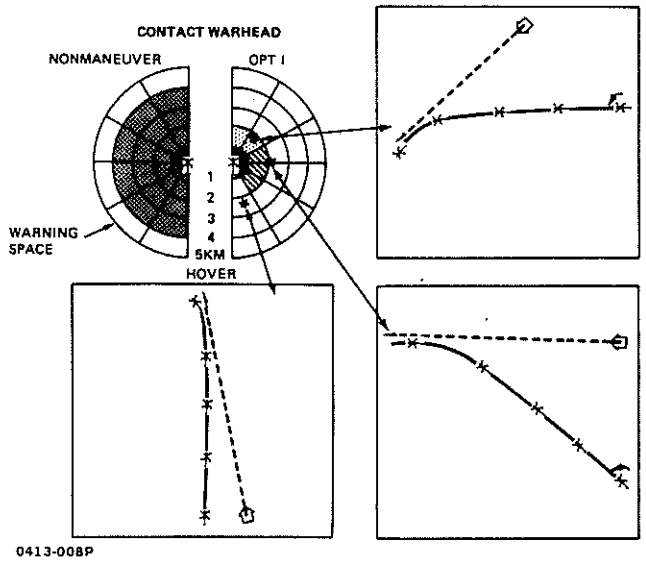

Figure 8. Evasive Maneuvers (From Hover)

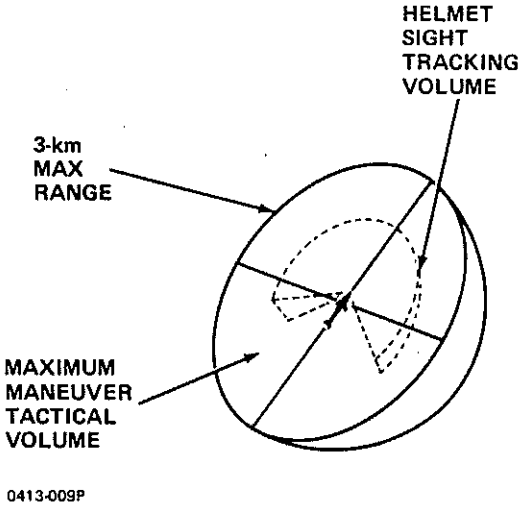

Figure 9. Visual Model

The maximum maneuver volume of each combatant is decomposed into a finite set of tactical contigencies by an assignment of thresholds involving the relative positions, velocities, and other observables during the combat. For the constant altitude maneuvering model, each combatant is assumed to measure relative range, angle off and relative heading as depicted in Fig. 10. Relative range has been divided into 5 cells from zero to 3 km; angle-off into eight 45° sectors from 0° around the compass to 360°; and relative heading divided into the four quadrants as shown in Fig. 10. These thresholds divide the maximum maneuver volume into 160 contingencies for the constant altitude combat case.

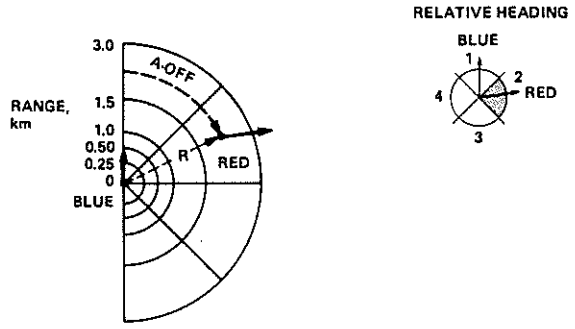

OBSERVABLES	# THRESHOLDS
• RELATIVE RANGE	(5)
• ANGLE OFF	(8)
• RELATIVE HEADING	(4)
• RELATIVE SPEED	(3)
• RELATIVE ALTITUDE	(3)

} CONSTANT ALTITUDE CASE 160 CONTINGENCIES

0413-010P

Figure 10. Maximum Maneuver Volume Thresholds

3.2 GUN MODEL

Both blue and red aircraft are assumed to be equipped with a turreted gun with target tracking accomplished by a helmet mounted sight. Fire control lead prediction employing target range, range rate, angular rate in flight data together with specific projectile ballistics is considered in the armament simulation. Depending upon the gun and projectile, a firing opportunity requires satisfaction of the following: target entry into the tracking volume; a "pipper" settle time delay associated with entry; and target range within a prespecified maximum firing range.

The probability of kill associated with an N-shot gun burst is developed from single shot considerations as follows:

SINGLE SHOT

$$P_{K_{SS}} = \frac{A_V}{2\pi\,(TERMX \cdot TERMY)^{1/2}} \cdot \exp\left\{-\frac{1}{2}\left[\frac{dx^2}{TERMX} + \frac{dy^2}{TERMY}\right]\right\}$$

- $TERMX = \sigma_D^2 + \sigma_{TX}^2 + \frac{A_V}{2\pi}$
- $TERMY = \sigma_D^2 + \sigma_{TY}^2 + \frac{A_V}{2\pi}$
- A_V GIVEN FOR SPECIFIC VIEWS

N-SHOT BURST

$$P_{K_N} = 1 - (1-P_{K_{SS}})^N$$

In the above σ_D is the dispersion error of the projectile; σ_{TX}, σ_{TY} the composite target tracking errors in x, y coordinates; and A_V the ballistic vulnerability of the aircraft to the threat projectile (measured in terms of vulnerable area). Other N-shot vulnerability models (such as the salvo fire model) have been employed in these studies without alteration of the basic methodology but are not reported here. In the computational results to follow both blue and red aircraft were assumed equipped with a 25 mm gun. The respective vulnerabilities of the aircraft are given in Table 1 for that threat projectile. The areas have been normalized by the numerical value of the vulnerable area in the side aspect for the baseline aircraft. The N-shot burst probability of kill for each combatant is employed at each step in the trajectory numerical integration process to determine the termination event; kill by red, kill by blue, mutual kill, and no kill by either.

Table 1. Aircraft Relative Vulnerability

ATTACK ASPECT / A/C	FRONT	SIDE	REAR	BOTTOM	TOP
BASELINE	.18	1.0	.22	.64	.59
LHX	.25	.76	.27	.71	.72
LHX/VR	.088	.27	.096	.26	.26
RED	.24	.75	.17	.47	.77

3.3 MANEUVER STRATEGY DEVELOPMENT

The constant altitude maneuver strategy for both combatants employs the elemental maneuver set labled control set I in Fig. 4. The associated maximum maneuver capabilities of the blue and red aircraft are summarized in Fig. 11. The transient response of all combatants to maximum commanded rates or accelerations is represented by a family of first order models as shown at the lower right of Fig. 11. The time constant associated with longitudinal commands is given by TAUPIT; load factor turn commands by TAUROL; and pedal turn commands by TAUYAW.

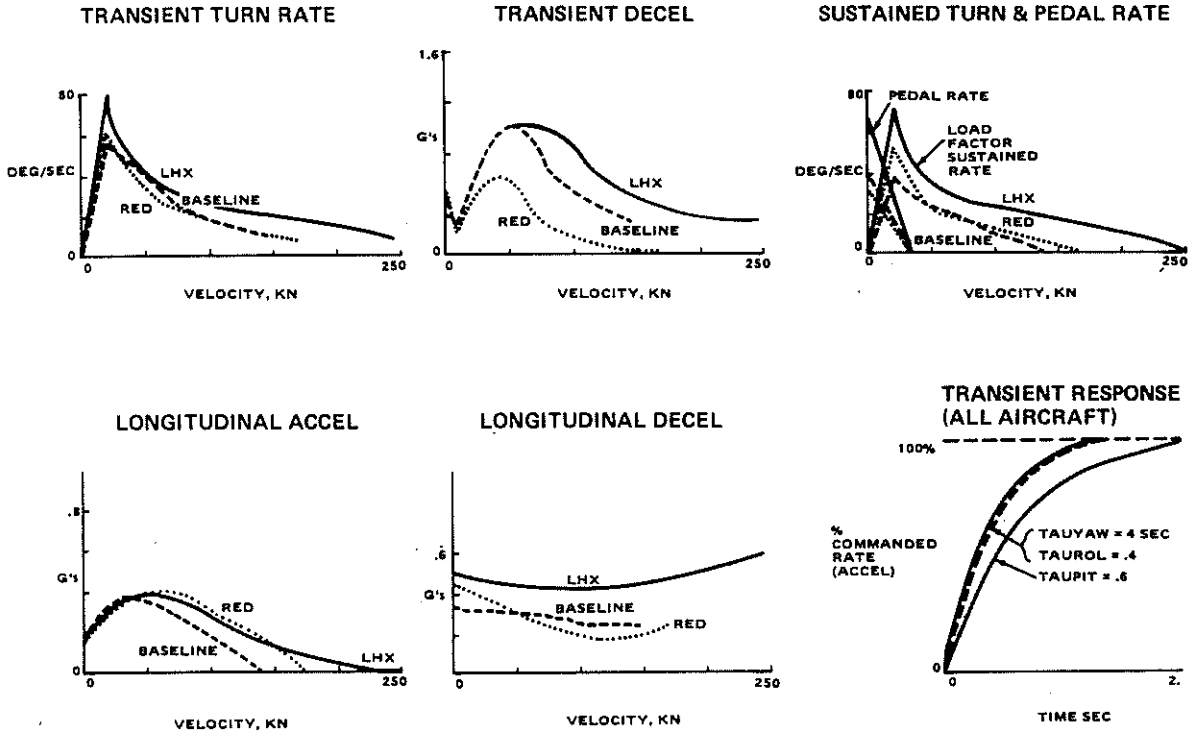

Figure 11. Sea Level Maximum Maneuver Performance

Each combatant's maneuvering strategy is represented by a choice of an elemental maneuver for each contingency cell of the maximum maneuver volume shown in Fig. 9. The stochastic learning methodology is easily extended to the two combatant case as depicted in Fig. 12. In contrast to the single decision table described in the missile avoidance application of Fig. 3, a blue and red decision table are now sequentially modified to produce optimal maneuver strategies for both combatants.

3.4 MANEUVER PERFORMANCE AND ARMAMENT EFFECTIVENESS

The one-on-one gun combat problem requires that one determine the domains of combat initial conditions (positions, velocities) for which each of the combatants has a unilateral capability in deciding the outcome of the combat. The comparative size of these domains furnishes a quantitative measure of superiority of one system over the other. To determine these domains, the computational method is first employed with each side maximizing his kill probability, and secondly, with one combatant maximizing kill probability with the other maximizing survivability. These separate solutions determine domains where each helicopter is best operated offensively, and where each should operate defensively with survivability as the main goal. Each of the computational results emerging from the stochastic learning solution methodology is presented in terms of a discretized initial condition space centered on the blue combatant as shown in Fig. 13. The probabilities of kill for each combatant and other important terminal statistics are computed for each discretized initial condition region as shown.

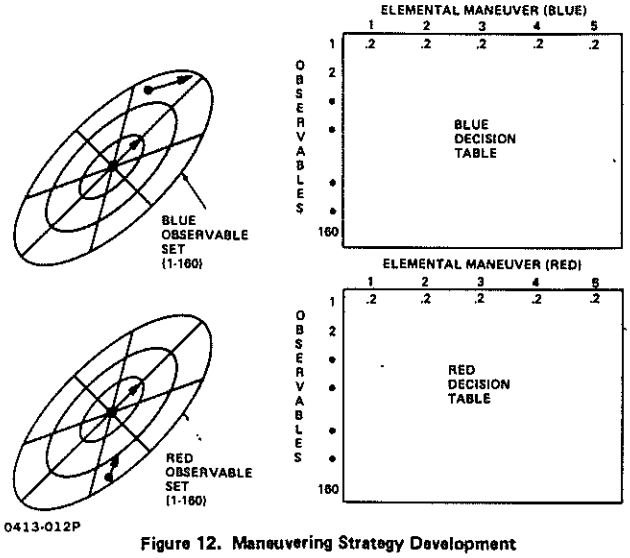

Figure 12. Maneuvering Strategy Development

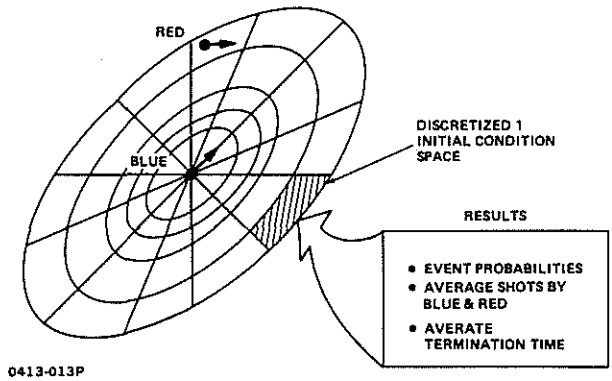

Figure 13. Format for the Computational Results

Two representative computational solutions employing the initial condition polar format of Fig. 13 are given in Figs. 14 and 15. The optimal solution in Fig. 14 considers the case of the blue LHX aircraft in an unarmed defensive role against an offensive red adversary equipped with a 25 mm, 1500 spm turreted gun. This solution considers combat initial speeds of 87 kn (45 m/s) for both combatants with both helicopters employing sustained turn for their load factor turn elemental maneuver choices. The four half-polar charts (due to initial condition symmetry) give the probability of kill for red in terms of relative range, angle-off, and relative heading. The half-polar at upper right corresponds to the coincident heading case, as schematically represented by the B and R vectors in the small auxiliary diagram. The remaining three heading cases are interpreted with the aid of the rotated R vector in the auxiliary diagrams. The cells of high kill probability for Red (P_{K_R}) are shaded according to the accompanying legend. The solution in Fig. 15 considers the LHX in the offensive role against an offensive red adversary for the same initial speed case of 87 kn (45 m/s). The LHX is equipped with identical turreted gun armament and fire control as the threat helicopter. The initial condition cells of high kill effectiveness are shown for each combatant using the P_{K_B}, P_{K_R} legend as indicated.

A more compact bar summary format enabling convenient combat effectiveness comparisons between helicopter/armament systems is shown in Fig. 16. The total of high kill and mutual kill area for both combatants as a percent of total area within a fixed radius of initial conditions for Fig. 15 is now plotted on the vertical scale at the right. The fixed radius is taken as 1.5 km representative of ranges associated with chance encounter initiation of helicopter engagements. The data shown in the circles at top and bottom of the bar graph indicate the average shots/kill achieved by each combatant in the high kill and mutual kill areas. The per cent of total initial area dominated by each combatant is a quantitative measure of his combat effectiveness or air superiority.

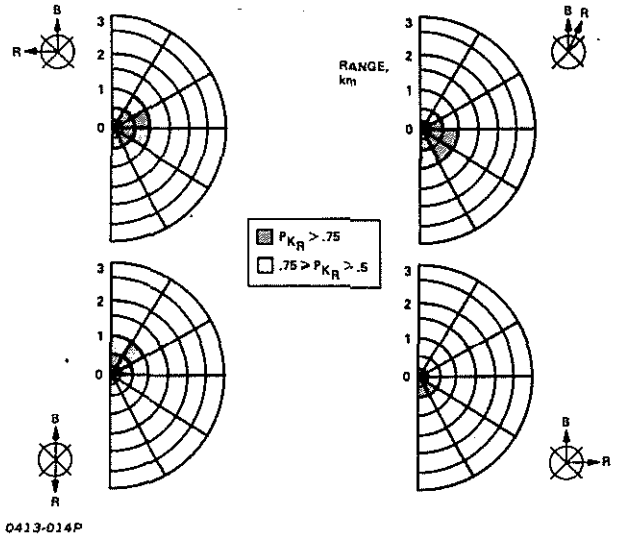

Figure 14. LHX Defensive Solution, 87 kn

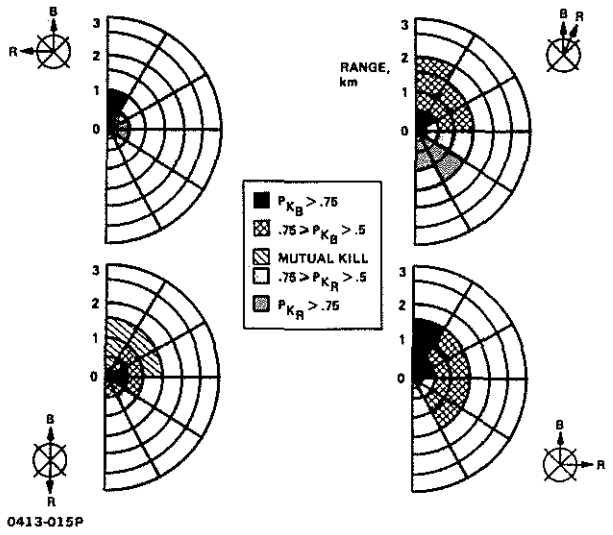

Figure 15. LHX Offensive Solution, 87 kn

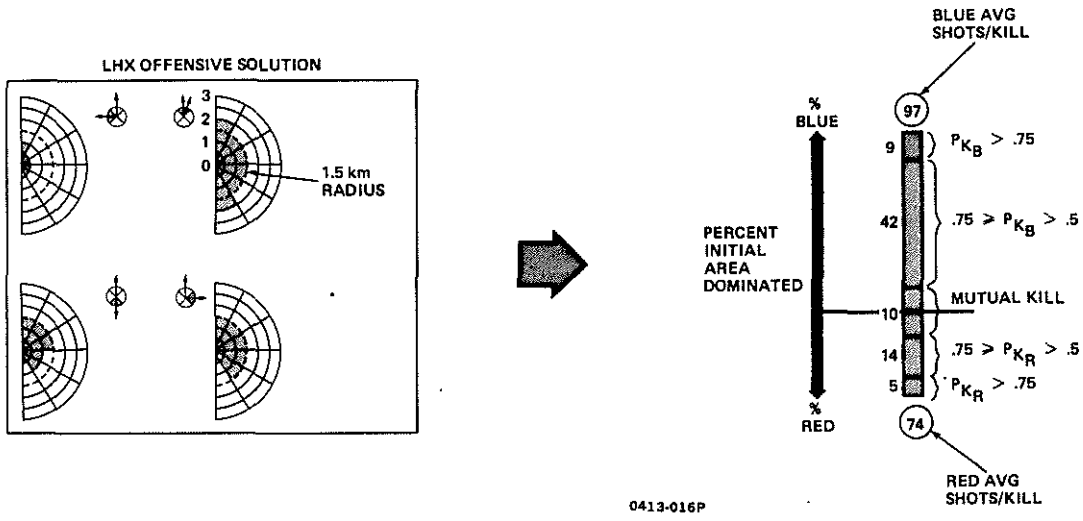

Figure 16. Bar Summary Format

A comparison of combat effectiveness of the baseline and LHX aircraft including variations in ballistic hardening, gun mount, and shot rate characteristics is shown in Fig. 17. All solutions shown are for combat initiated at 87 kn (45 m/s) for both combatants with maximum sustained turn capability employed as the load factor turn elemental maneuver choice. The first three bar graphs (from the left) correspond to defensive solutions for various blue helicopters against the offensive red adversary. The red threat employs a 25 mm, 1500 spm, turreted gun with ± 90 degree azimuth capability, and +21° and -50° elevation capability. The reduction in red kill effectiveness achieved by the more maneuverable LHX and LHX with ballistic hardening can be compared with the baseline aircraft.

Bar graphs four through nine consider various blue aircraft/armament configurations in an offensive role against the offensive threat previously described. In the fourth case, labeled (LHX/FLEX) the LHX aircraft was equipped with a limited sweep (± 6° elevation and azimuth) gun mount. The composite tracking error standard deviation in this case was assumed to be $\sigma_{TX} = \sigma_{TY} = 6$ mil and the projectile dispersion $\sigma_D = 5$ mil. The gun caliber and shot rate were assumed equivalent to that employed by the threat. (Note: for all 25 mm turreted gun applications, both blue and red, the composite tracking error was assumed to be $\sigma_{TX} = \sigma_{TY} = 20$ mil and the dispersion $\sigma_D = 5$ mil). The low shots/kill by blue reflects the smaller ammunition expenditure obtained by the assumed 6 mil error fire control tracking error performance of a limited sweep HUD system.

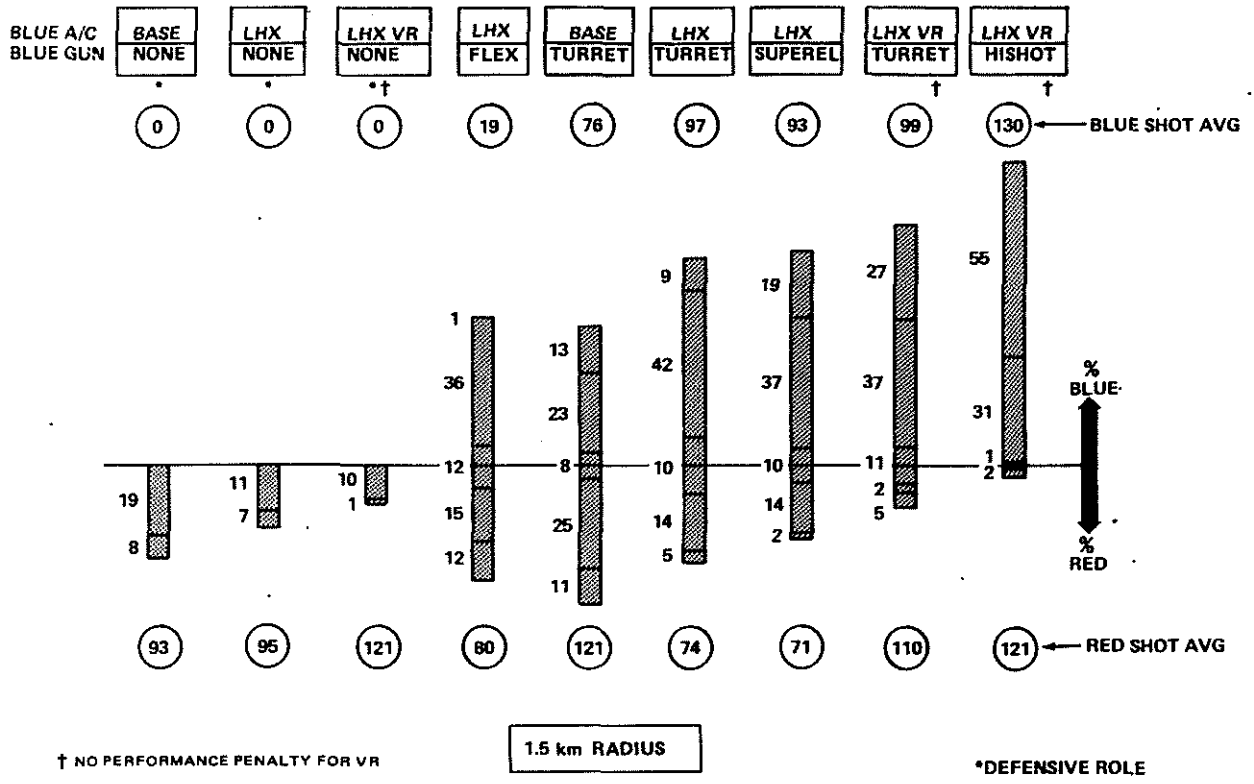

0413-017P

Figure 17. Helicopter/Armament Combat Effectiveness Comparisons

The fifth column corresponds to the base line helicopter equipped with the same turreted gun as the red adversary. The % area ratio for measuring dominance is nearly 1:1 against red. The sixth column shows the LHX capability with the same turreted gun against the threat. The gain in combat effectiveness of the higher maneuverability LHX compared to the baseline is appreciable, but is somewhat offset by the higher ballistic vulnerability of the LHX. Column seven quantifies the gains achievable by the LHX if superelevation of the turreted gun to +50° were permissible (rather than +21° because of rotor clearance). Bar graph eight illustrates the impact of ballistic hardening improvements to the turreted gun LHX. Comparison with the standard LHX results in column six, indicates an appreciable reduction in the kill effectiveness area of red, while improving the % area of highest kill probability (9% improved to 27%). The last column on the right illustrates the high combat effectiveness achieved with a 3000 spm turret gun equipped LHX design incorporating ballistic hardening. These results illustrate the significant interdependence of maneuverability, armament, and ballistic hardening factors for friendly and threat helicopters that enter the combat effectiveness evaluation.

3.5 LHX MANEUVER EFFECTIVENESS

In the design concept phase, it is often important to quantify the sensitivity of combat effectiveness to maneuver parameter variations on a one at a time basis while holding other aircraft and armament parameters fixed. As an example of this, the original sea level maximum longitudinal acceleration parameter of the LHX (labeled LHX A in Fig. 18) was enhanced to that given by the function labeled LHX B. All other maneuver performance, ballistic hardening, and armament parameters were held fixed. The corresponding improvement in combat effectiveness for the blue offensive/red offensive case for the 87 kn (45 m/s) initial speed is shown in Fig. 19. The bar graph on the left is the result originally obtained for the LHX turret case first illustrated in Fig. 17.

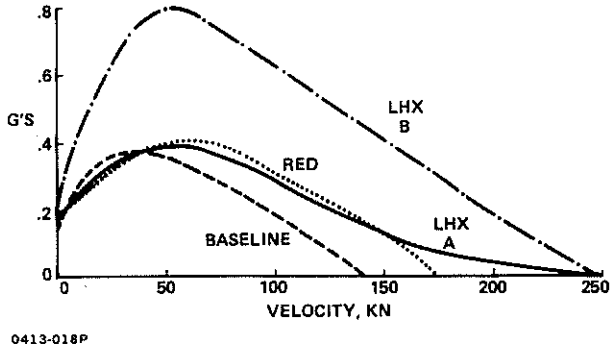

Figure 18. Sea Level Maximum Longitudinal Acceleration Variation

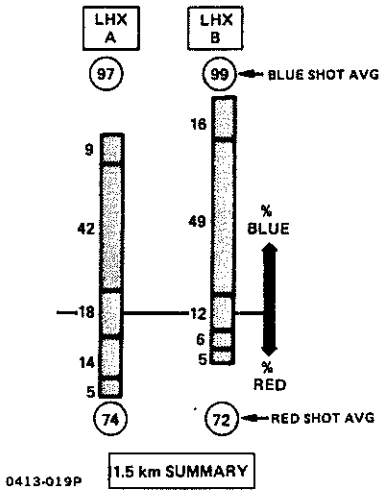

Figure 19. Sensitivity of Combat Effectiveness

4. CONCLUSIONS

This paper has sketched the development and application of a digital simulation technique incorporating optimization and game theory concepts for assessment of helicopter performance in air-to-air combat. The numerical experience to date suggests that a respectable amount of detail regarding the integrated use of maneuver, threat warning, ballistic hardening, and armament capability can be considered in design studies and that combat effectiveness assessments can be accomplished with reasonable computer time budgets.

Although the results show that combat effectiveness is strongly dependent upon the integrated use of the above factors, a maneuver performance advantage can provide sizable gains in survivability in the defensive role and kill effectiveness in the offensive role. The results presented here have combat maneuvers limited to constant altitude, however, similar computational models which include vertical plane maneuvering are currently under investigation with results available in the near future.

5. ACKNOWLEDGEMENTS

The authors would like to thank the following personnel and their organizations for their technical contributions in the development of the helicopter/armament system computer models utilized in these studies:

Dr. L. Feaster; U.S. Army AVRADCOM, St. Louis, MO

Mr. J. Means; Hughes Helicopters, Culver City, CA

Mr. E. V. Merritt and Mr. J. Anderson; U.S. Army AVRADCOM, Ft. Eustis, VA

Mr. P. Townsend and Mr. T. Hung; U.S. Army ARRADCOM, Dover, N.J.

Mr. R. Bruce and Mr. J. Wagner; General Electric Co., Burlington, VT

Mr. F. Sobierajski and Mr. H. Hinz; Grumman Aerospace Corp., Bethpage, NY

6. REFERENCES

1. Issacs, R., Differential Games, John Wiley, New York, 1965.

2. Breakwell, J.V. and Merz, A.W., Toward a complete solution of the homicidal chauffeur game, Proceedings of the First International Conference on Theory and Applications of Differential Games, Amherst, Mass., Oct 1969.

3. Baron, S., Kleinman, D., Serben, S., A study of the markov game approach to tactical maneuvering problems, NASA Report CR-1979, Feb 1972.

4. Falco, M., Cohen, V., Strategy synthesis in aerial dogfight game models, AIAA 11th Aerospace Sciences Meeting, Washington, D.C., AIAA Paper 73-233, Jan 1973.

5. Falco, M., and Carpenter, G., Survivability analysis of air and land vehicles to missile threats, 4th Symposium on Vulnerability and Survivability, American Defense Preparedness Association, Tyndall AFB, Florida, March 1979 (and Grumman Research Department Memorandum).